

## Supporting Information

# Doping Ultrasmall Cubic ZnS Nanocrystals with $\text{Mn}^{2+}$ Ions over a Broad Nominal Concentration Range

Sergiu V. Nistor, Mariana Stefan, Leona C. Nistor, Daniela Ghica,

Ioana D. Vlaicu and Alexandra C. Joita

National Institute of Materials Physics, str. Atomistilor 105 bis,

Magurele-Ilfov, RO-077125, Romania

### A. Structure and EPR properties of cZnS NCs prepared without Tween 20 surfactant

The XRD pattern of the cZnS:Mn (20000 ppm) sample prepared without Tween 20 surfactant (Fig. S1, curve a) is practically identical with the pattern of the similar sample prepared in standard conditions<sup>1</sup> (Fig. 1a from the article), resulting from a cubic (sphalerite) structure of NCs of 2.9 nm average core diameter and lattice parameter  $a = 0.5393 \pm 0.0002$  nm.

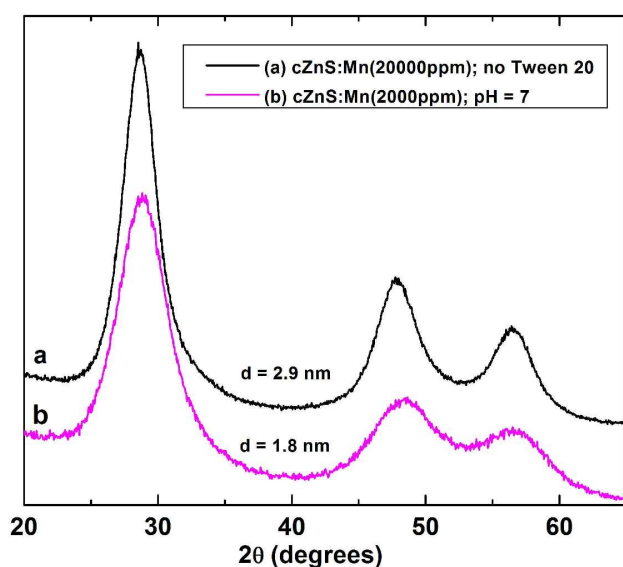


**Fig. S1:** The XRD patterns of cZnS:Mn NCs; (a) Doped with 20000 ppm  $\text{Mn}^{2+}$  ions, prepared without Tween 20 surfactant. (b) Doped with 2000 ppm  $\text{Mn}^{2+}$  ions, prepared with Tween 20 surfactant at higher pH = 7.

The HRTEM image (Fig. S2) confirms the presence of aggregates of cZnS:Mn NCs of approximately 3 nm average size, self-assembled in the final step of the synthesis.<sup>1</sup> Compared to the cZnS:Mn (20000 ppm) sample prepared in standard conditions (see Fig. 1d from the article) the sample prepared without Tween 20 surfactant exhibits a tighter aggregation. Stacking defects are again visible in the component nanocrystallites marked by A and B in Fig. S2. Such planar defects can be imaged in HRTEM at atomic resolution only if they exhibit translation symmetry along the viewing direction. For cZnS crystals this condition is fulfilled along the [110] viewing direction, *i. e.* stacking faults or twins can be revealed only for the NCs oriented along the [110] zone axis.

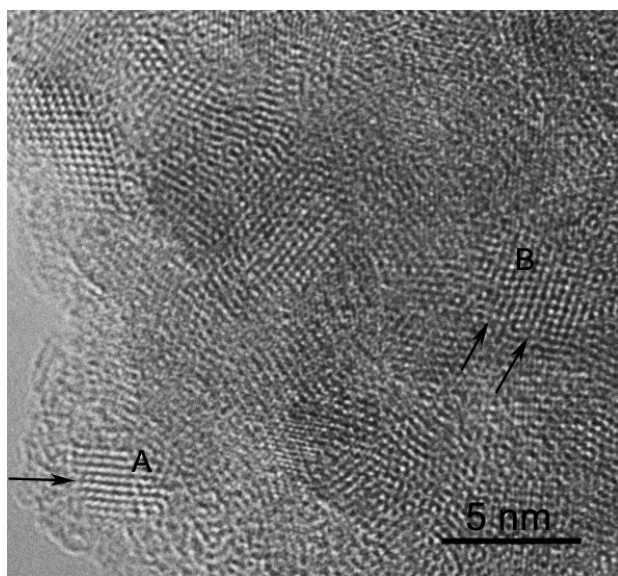


**Fig. S2.** *HRTEM image of the cZnS:Mn (20000 ppm) NCs, prepared without Tween 20 surfactant. The NCs are self-assembled in a tighter mesoporous structure. Black arrows indicate the dislocation steps at the surface of a few component cZnS NCs.*

The examination of Fig. S2 reveals that many such well oriented NCs contain one or more stacking defects, which cross the whole nanocrystallite core and emerge in dislocation steps at the surface of the NCs. The resulting surface steps are indicated in Fig. S2, as well as in Fig. 1d from the article, by black arrows. According to the ELDA mechanism of impurity incorporation,<sup>2</sup> they represent trapping sites for the incorporation of the  $\text{Mn}^{2+}$  impurity ions during the cZnS NCs growth.

The X-band EPR spectrum of the cZnS:Mn (20000 ppm) sample prepared without Tween 20 surfactant is presented in Fig. S3, together with the spectrum of a sample prepared in standard conditions at the same doping level. Although the two spectra are comparable with regard to the shape of the three EPR component lines, the intensity is larger for the sample prepared without Tween 20 surfactant.

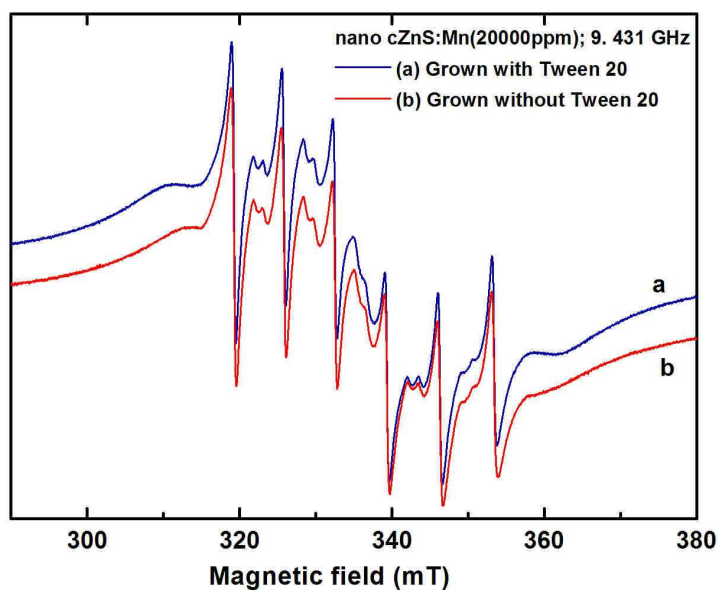


**Fig. S3.** The X-band EPR spectra of the cZnS:Mn (20000 ppm) NCs, prepared in standard conditions: (a) with Tween 20 surfactant and (b) without Tween 20 surfactant. Spectra were recorded in identical conditions and normalized for the same quantity of cZnS:Mn.

### B. Structure and EPR properties of cZnS:Mn NCs prepared at higher pH = 7

According to the XRD data (Fig. S1, curve b) the cZnS sample prepared at higher pH = 7 consists of cZnS NCs of 1.8 nm average core diameter and lattice parameter  $a = 0.5372 \pm 0.0002$  nm. The HRTEM image (Fig. S4) confirms the presence of cZnS NCs of smaller core diameter compared to the samples prepared in standard conditions, at pH = 5.5 (see Fig. 1d from the article). Moreover, the smaller cZnS NCs are separated by a thick layer of disordered

nanomaterial, very likely hosting the surface bound  $\text{Mn}^{2+}$  ions. As in the other investigated samples, a rather large proportion of the NCs contain stacking defects.

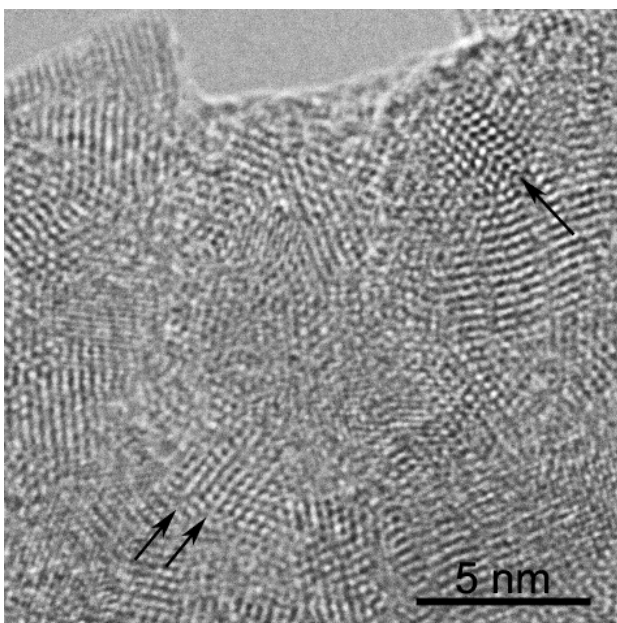


**Fig. S4.** HRTEM image of an aggregate of  $\text{cZnS:Mn}$  (2000 ppm) NCs, prepared in standard conditions, but at higher  $\text{pH} = 7$ . The individual  $\text{cZnS}$  NCs are separated by a thicker layer of disordered material. Black arrows indicate dislocation steps produced by the stacking defects emerging at the NCs surface.

Further information about the composition of the disordered material separating the  $\text{cZnS}$  NCs was obtained from the analysis of the EPR spectra (Figs. S5 and S6). One should mention that, due to the relatively low concentration of incorporated  $\text{Mn}^{2+}$  ions, the component lines of the surface localized  $\text{Mn}^{2+}$  ions, which cannot be easily observed in the X-band spectra (Fig. S5), are better observed in the Q-band spectra (Fig. S6). Thus, one finds a clear difference in the hyperfine splitting  $A$  of the surface localized  $\text{Mn}^{2+}$  ions in the two samples, reflecting changes in the nature and configuration of the ligands bound to the surface / shell localized  $\text{Mn}^{2+}$  ions in the two cases.<sup>3</sup> This is better seen in the total separation  $\Delta A$  between the extreme hyperfine components.

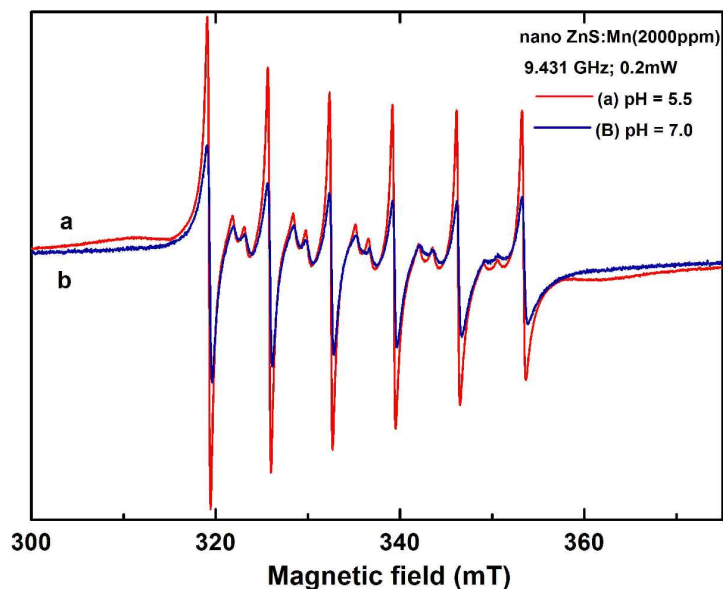


**Fig. S5.** X-band EPR spectra recorded in identical conditions of cZnS:Mn (2000 ppm) NCs: (a) prepared in standard conditions, at pH = 5.5, (b) prepared at pH = 7.

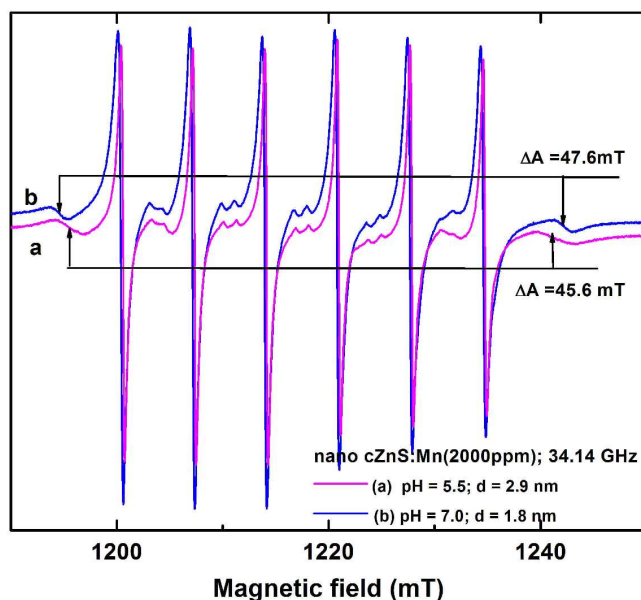


**Fig. S6.** Q-band EPR spectra of the cZnS:Mn (2000 ppm) NCs: (a) prepared in standard conditions, at pH = 5.5, (b) prepared at pH = 7. The extreme hyperfine lines from the Mn<sup>2+</sup> ions localized on the surface are indicated by arrows.

The corresponding SH hyperfine parameter  $A = -89 \times 10^{-4} \text{ cm}^{-1}$  determined for the NCs prepared at pH = 7.0 is larger than the hyperfine parameter value  $A = -84.5 \times 10^{-4} \text{ cm}^{-1}$ , determined for the  $\text{Mn}^{2+}$  ions localized on the surface of the cZnS:Mn NCs prepared at pH = 5.5 in standard conditions. It is also larger than the value  $A = -86.9 \times 10^{-4} \text{ cm}^{-1}$  determined for the  $\text{Mn}^{2+}$  ions localized in a  $\epsilon\text{-Zn(OH)}_2$  shell,<sup>3</sup> coordinated by four  $\text{OH}^-$ , suggesting a six-fold coordinated oxy-hydrated structure of the disordered host/shell. Meanwhile the hyperfine parameter  $A = -84.5 \times 10^{-4} \text{ cm}^{-1}$ , determined for the  $\text{Mn}^{2+}$  ions localized on the surface of the cZnS:Mn NCs prepared at pH = 5.5, is close to the value  $A = -84.7 \times 10^{-4} \text{ cm}^{-1}$  determined for the  $\text{Mn}^{2+}$  ions localized in the hydrozincite, at  $\text{Zn}^{2+}$  sites six-fold coordinated by four  $\text{OH}^-$  groups and two  $\text{O}^{2-}$  ions from  $\text{CO}_3$  groups.<sup>4</sup> These results suggest a mixed bonding to surface adsorbed  $\text{H}_2\text{O}$  and  $\text{CO}_2$  molecules for the surface bound  $\text{Mn}^{2+}$  ions.

## References

- (1) Nistor, L. C.; Mateescu, C. D.; Birjega, R.; Nistor, S. V. Synthesis and Characterization of Mesoporous ZnS with Narrow Size Distribution of Small Pores. *Appl. Phys. A* **2008**, *92*, 295-301.
- (2) Nistor, S. V.; Stefan, M.; Nistor, L. C.; Ghica, D.; Mateescu, C. D.; Barascu, J. N. Defect Assisted Incorporation of  $\text{Mn}^{2+}$  Ions in Cubic II-VI Semiconductor Quantum Dots. *IOP Conf. Ser.: Mater. Sci. Eng.*, **2010**, *15*, 012024 1-7.
- (3) Nistor, S. V.; Ghica, D.; Stefan, M.; Nistor, L. C. Sequential Thermal Decomposition of the Shell of Cubic ZnS/ $\text{Zn(OH)}_2$  Core-Shell Quantum Dots Observed with  $\text{Mn}^{2+}$  Probing Ions. *J. Phys. Chem. C* **2013**, *117*, 22017-22028.
- (4) Nistor, S. V.; Nistor, L. C.; Stefan, M.; Ghica, D.; Aldica, Gh.; Barascu, J. N. Crystallization of Disordered Nanosized ZnO Formed by Thermal Decomposition of Nanocrystalline Hydrozincite. *Cryst. Growth Des.* **2011**, *11*, 5030-5038.